



Comment on "Techno-economic analysis of capacitive and intercalative water deionization" by M. Metzger, M. Besli, S. Kuppan, S. Hellstrom, S. Kim, E. Sebti, C. Subban and J. Christensen, *Energy Environ. Sci.*, 2020, 13, 1544

Journal:	<i>Energy & Environmental Science</i>
Manuscript ID	EE-CMT-10-2020-003321.R1
Article Type:	Comment
Date Submitted by the Author:	06-Dec-2020
Complete List of Authors:	Patel, Sohum; Yale University, Chemical and Environmental Engineering Wang, Li; Yale University, Department of Chemical and Environmental Engineering Elimelech, Menachem; Yale University, Department of Chemical and Environmental Engineering

Comment on Article

Comment on “Techno-economic analysis of capacitive and intercalative water deionization” by M. Metzger, M. Besli, S. Kuppan, S. Hellstrom, S. Kim, E. Sebti, C. Subban and J. Christensen, *Energy Environ. Sci.*, 2020, 13, 1544

Energy & Environmental Science

Revised: December 6, 2020

Sohum K. Patel, Li Wang, and Menachem Elimelech^{a*}

*^aDepartment of Chemical and Environmental Engineering, Yale University, New Haven,
Connecticut 06520, United States*

*Corresponding Author; Address: P.O. Box 208268, Yale University, New Haven, CT 06520; Email: menachem.elimelech@yale.edu; Phone: +1 (203) 432-2789; Fax: +1 (203) 432-2881

1 A recent publication in *Energy & Environmental Science* by Metzger et al.¹ presented a techno-
2 economic analysis of electrochemical water desalination technologies, specifically focusing on
3 membrane capacitive deionization (MCDI), hybrid capacitive deionization (HCDI), and
4 intercalative deionization (IDI). In their analysis, the authors predicted the capital investment as
5 well as the operational costs, with the latter assumed to be based on the energy consumption of
6 desalination. Ultimately, the study concludes that IDI is highly promising, largely based on the
7 claim of superior energy efficiency with respect to other desalination technologies. However, the
8 energy consumption analysis performed in this study is overly simplified, compromising the
9 validity of the technological comparison. In this Comment, we discuss the issues in the applied
10 method of comparing energy consumption among technologies and provide a corrected approach
11 with new results for a more valid comparison.

12 The focus of our Comment is in regards to Figure 6 of the article, in which the authors show
13 the “energy efficiency”, \hat{E}_{fresh} , of multiple desalination technologies as a function of feedwater
14 salt concentration. We note that the term “energy efficiency” is improperly utilized, with energy
15 efficiency in the context of desalination processes typically referring to the second-law efficiency,
16 which compares the actual energy consumption to the thermodynamic minimum energy
17 consumption.²⁻⁵ Rather, \hat{E}_{fresh} , defined as the energy spent per unit of freshwater produced, is
18 more appropriately referred to as the specific energy consumption⁶ for the remainder of the
19 discussion.

20 Through Figure 6, the authors aim to compare the specific energy consumption of several
21 desalination technologies across a wide range of feed concentrations. Particularly, salinities
22 ranging from 100 ppm to 100,000 ppm NaCl are shown, encompassing the brackish water and
23 seawater ranges. A critical shortcoming of Figure 6, however, is that the particular separation
24 parameters for the presented data are not specified. To compare various desalination technologies
25 fairly, the desalination separation parameters — namely, the feed salinity, extent of salt removal,
26 and water recovery — must be held consistent, though in Figure 6, the authors provide only the
27 feed salinity. Nonetheless, it can be inferred from the reported energy consumptions that the
28 separation parameters are not unified across technologies. Such an approach is highly problematic
29 since RO inherently removes extensive amounts of salt (>99%) across all feed salinities, whereas
30 CDI-based technologies are generally operated with significantly lower salt removals, especially

31 when higher feed salinities are treated.^{2, 7, 8} Hence, when the separation parameters are not held
32 consistent, the energy consumption of RO would be inflated with respect to CDI, as it is used to
33 perform a more “difficult” water-salt separation. Similarly, the productivity — the rate of water
34 production per mass transfer area — must be fixed among the technologies to ensure valid
35 comparison. Though the productivity does not directly affect the thermodynamic minimum energy
36 requirement,⁶ an increase in productivity generally demands a larger specific energy consumption
37 to facilitate the increased rate of mass transfer.^{9, 10} In Metzger et al., however, the productivity is
38 not considered.

39 In addition to the nonunified separation parameters and productivity, it is important to note that
40 the authors use overly simplified modeling techniques to predict the specific energy consumption
41 of each technology. The energy consumption of RO is adapted from Urban¹¹ and Oren¹², which
42 linearly extrapolate the specific energy consumption across the entire salinity range based on
43 values from actual desalination plants that include additional energy-consuming processes such as
44 intake, pre-treatment, and post-treatment.¹³ Furthermore, energy recovery, despite being
45 commonly practiced in RO, is not considered.¹²

46 The CDI modeling performed in Metzger et al. is also highly empirical, largely depending on
47 the system geometry, internal resistance values, and cell voltage profiles (over a charge-discharge
48 cycle) from only a few experimental studies conducted under particular operating conditions and
49 separation parameters. Specifically, the authors calculate the energy consumption of each of the
50 CDI processes according to (eq 18 in the original paper)

$$E_{charge} = I_{charge} \int_0^{t_{charge}} E_{cell} dt \quad (1)$$

51 where I_{charge} is the required current to achieve a given extent of salt removal, t_{charge} is the time of
52 the charging step, and E_{cell} is the cell voltage.

53 For the I_{charge} , the authors assume a fixed charge efficiency value of 0.92. Though such a charge
54 efficiency is reasonable for relatively low feed salinities and extents of salt removal,⁴ the authors
55 extend this value into their modeling of the entire brackish water and seawater regimes. The actual
56 charge efficiency in CDI, however, is known to considerably vary with the feed salinity and the
57 cell potential.^{14, 15}

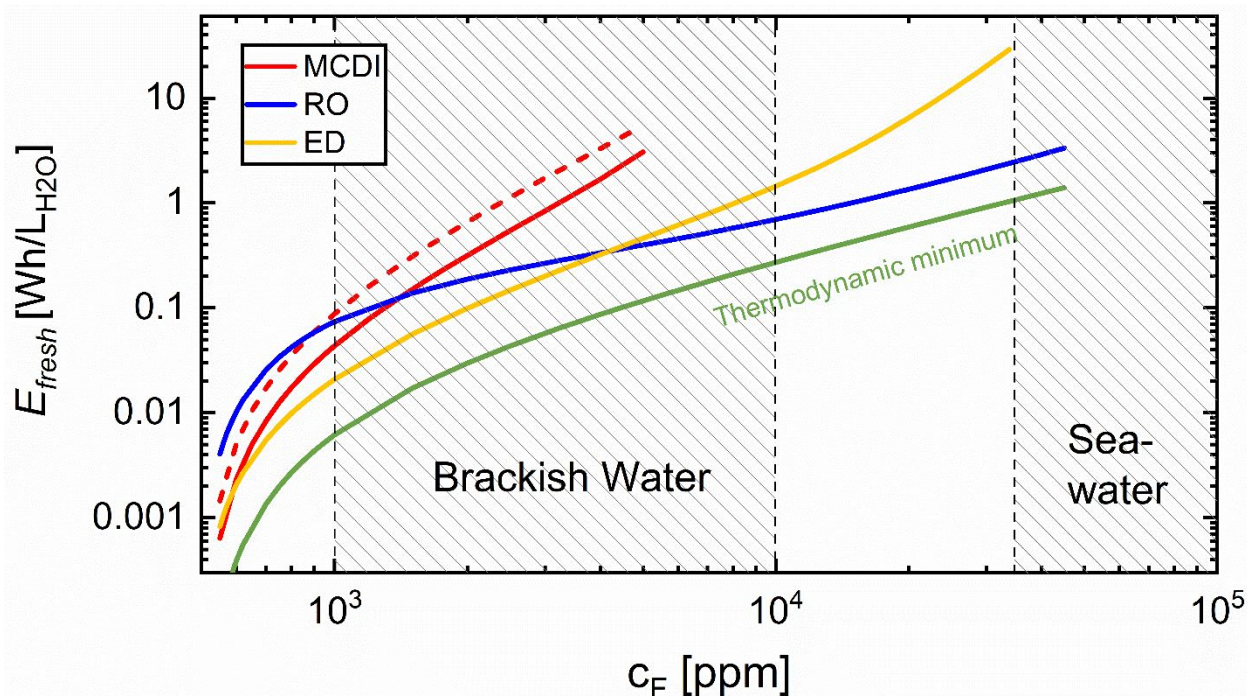
58 The authors also simplify the determination of E_{cell} and its time dependence by only taking the
59 iR corrected voltage profiles from three experimental studies — one for each CDI technology (i.e.,
60 MCDI, HCDI, IDI). These voltage profiles are then extended across the entire feed salinity range
61 according to the determined I_{charge} and the fixed internal resistance value, R_{mod} . The cell voltage
62 in actual CDI operation, however, is highly dependent on several parameters including the feed
63 salinity, extent of salt removal, salt removal rate, and electrode properties. Therefore, the approach
64 taken by the authors is likely to lead to major error in the determination of energy consumption.

65 In addition, the modeling of energy recovery in Metzger et al., in which a fixed energy recovery
66 ratio (ER) is utilized across all simulated separation parameters and operating conditions, is
67 erroneous and overly simplified. It has been demonstrated that the fraction of potentially
68 recoverable energy in MCDI is highly dependent on the internal cell resistances, the feed salinity
69 and extent of salt removal, and the operating conditions during both the charge and discharge step
70 (i.e., current density and flowrate).^{16, 17}

71 As a result of the simplifying assumptions made by the authors, each of the CDI performance
72 lines presented in Figure 6 show a simple linear trend across the entirety of the feed salinity range
73 presented, though in actuality non-ideal transport phenomena such as concentration polarization
74 and co-ion leakage lead to deviation from such behavior.^{10, 18-20} Furthermore, without the
75 specification of the separation parameters, which set the thermodynamic minimum energy
76 consumption,⁶ the presentation of a thermodynamic minimum energy consumption line is illogical.
77 However, the authors show a line for the thermodynamic minimum energy consumption (\hat{E}_{min}),
78 adapting it from values reported in previous studies, rather than properly calculating it for variable
79 separation parameters.

80 Due to the abovementioned issues in the energy analysis performed by Metzger et al., the
81 conclusions drawn in the article based on Figure 6 must be reevaluated. Particularly, the authors
82 state that the energy consumption of MCDI is lower than RO and electrodialysis (ED) across the
83 entire brackish water range, in direct contrast with the findings of previous works, which show RO
84 and ED are considerably more energy efficient than MCDI for brackish water desalination.^{2, 19, 20}
85 Hence, in Figure 1 we present a revised version of Metzger et al.'s Figure 6 to demonstrate the
86 vastly different results obtained upon correcting the described shortcomings of the energy analysis.
87 Specifically, we show the specific energy consumption of RO, ED, and MCDI, as well as the

88 thermodynamic minimum energy consumption for various feed salinities. Notably, the separation
 89 parameters are specified and unified across all technologies by fixing the product water salinity
 90 for all feed salinities (i.e., the extent of salt removal), water recovery, and productivity at 500 ppm,
 91 50%, and $15 \text{ L m}^{-2} \text{ h}^{-1}$, respectively. Though we do not directly simulate the performance of HCDI
 92 and IDI, we reiterate that the modeling approach taken by the authors for HCDI and IDI is the
 93 same as MCDI;¹ thus, error in the MCDI data suggests similar issues in the validity of the shown
 94 HCDI and IDI results.



95
 96 **Figure 1.** The specific energy consumption (\hat{E}_{fresh}) of desalination by MCDI (red), RO (blue), and ED
 97 (yellow) for varying feed salinities. The dashed red line indicates MCDI without energy recovery, whereas
 98 the solid line indicates the application of energy recovery with reverse current operation. The product water
 99 salinity is fixed at 500 ppm for all the feed salinities, while the water recovery and productivity are set at
 100 50% and $15 \text{ L m}^{-2} \text{ h}^{-1}$, respectively. The thermodynamic minimum energy requirement for each of the
 101 separation parameters is shown by the green line.

102
 103 Since RO membranes inherently operate with very high salt rejection, here we utilize a bypass
 104 system, as introduced in our previous study,¹⁹ in which only a portion of the feedwater is passed
 105 through the RO module — enabling variable salt removal for fair comparison with MCDI and ED.
 106 Feedwater which does not directly pass through the high-pressure pump and RO module is
 107 redirected to either a brine or product bypass stream. By mixing the product bypass stream with

108 the permeate from the RO module, the degree of salt removal can effectively be controlled. The
109 flow rates of the three streams are numerically optimized for each set of separation parameters to
110 minimize the specific energy consumption, using the module-scale water recovery as the variable
111 parameter. As is commonly practiced in RO, we apply an energy recovery device to recoup energy
112 stored in the retentate stream. Here, we assume an energy recovery device with 80% efficiency, a
113 relatively conservative value with respect to current state of the art pressure-exchangers.^{21,22} Mass
114 transfer modeling in the RO module is conducted using a classical solution-diffusion model, with
115 film theory applied to describe concentration polarization. Specified parameters for the RO model
116 can be found in Table 1 and further details regarding the RO bypass system modeling can be found
117 in our previous work.¹⁹

118 We note that in Figure 1, the presented curve for RO is not entirely linear, in contrast to Figure
119 6 of Metzger et al., in which the RO data across the entire feed salinity range was simply linearly
120 extrapolated.¹² Rather, because we employ a bypass system to achieve the necessary variable salt
121 removal for each feed salinity, we obtain a curve in which the initial rate of increase of \hat{E}_{fresh} for
122 RO is high, eventually steadying off to a more linear relation for the treatment of higher feed
123 salinities. This is a sensible result, as for low feed salinities ($<1 \text{ g L}^{-1}$), the extent of salt removal
124 required to achieve the fixed product water salinity (500 ppm) is small. Thus, most of the feedwater
125 is bypassed away from the RO module, and any small increase in the feed salinity leads to a
126 relatively large difference in the amount of water which must be directed to the RO module (which
127 is directly proportional to the required hydraulic pressure and energy consumption). When treating
128 feed salinities in the brackish water regime and beyond, in contrast, a sizeable portion of the
129 feedwater must be sent through the RO module to achieve the 500 ppm product water requirement,
130 making the trend (for a fixed product water salinity, productivity, and membrane water
131 permeability coefficient) increasingly linear.

132 To determine the energy consumption of ED, we use a previously demonstrated two-
133 dimensional Nernst-Planck modeling approach, thereby capturing the primary ion-transport
134 mechanisms of the ED process.^{20, 23-26} Specifically, the Nernst-Planck equation is numerically
135 solved in both the spacer channel and ion-exchange membranes with the assumption of
136 electroneutrality, allowing for the determination of the salt concentration and potential at each
137 point in the ED stack. Such an approach to ED modeling captures the effects of non-ideal

138 phenomena which are prevalent at high feed salinities and extents of salt removal, such as the
139 back-diffusion of ions from the concentrate channel to the diluate channel and the transport of co-
140 ions across ion-exchange membranes. The ED system is operated in single-pass continuous flow
141 mode, and assumed to be at steady state. ED modeling parameters utilized are shown in Table 1,
142 and further detail regarding the calculation of energy consumption can be found in the literature.^{20,}
143 ²⁴

144 In Figure 1, it can be seen that the \hat{E}_{fresh} curve of ED shows varying behavior according to the
145 feed salinity region. For feed salinities below the brackish water regime, the rate of change of
146 \hat{E}_{fresh} is highly variable. This is because at such low salt concentrations, the solutions in the spacer
147 channels pose high electrical resistance. In our analysis, we fix the product water concentration at
148 500 ppm, but the salinity in the concentrate channel varies, increasing with the feedwater
149 concentration. Thus, as the brackish water region is approached, the conductivity of the solution
150 in the concentrate channels increases, in effect diminishing the contribution of the concentrate
151 channel potential drop to the overall energy consumption. The rate of increase of \hat{E}_{fresh} , as a result,
152 begins to decline (i.e., “level-off”). For the treatment of brackish water, a steady rate of growth in
153 the energy consumption is observed, though when the feed salinity is further extended, the energy
154 consumption begins to show exponential-like growth. This increased growth rate in \hat{E}_{fresh} is the
155 result of the growing severity of concentration polarization and the large concentration differences
156 that develop across the ion-exchange membranes — both of which exacerbate the
157 counterproductive phenomena of back-diffusion and co-ion leakage, and effectively deteriorate
158 the current efficiency of desalination. We note that the \hat{E}_{fresh} curve of ED does not extend into the
159 seawater regime, as the high degrees of salt removal would require very large energy consumption
160 and the application of current densities which exceed the practical limiting current density (i.e.,
161 the current density which leads to zero concentration at the membrane surface on the diluate-side
162 due to concentration polarization) for such a single-stage operation.

163 Our modeling of MCDI, like ED, relies on the mechanistic description of ion-transport using
164 the Nernst-Planck equation, in addition to modified Donnan theory to describe the structure of the
165 electrical double layer. Such an approach is commonly adopted for MCDI modeling; hence, we
166 refer the reader to the literature for further detail.^{4, 15, 20, 27, 28} An MCDI cell is typically charged
167 under either constant current (CC) or constant voltage (CV) operation.²⁹ In this analysis, we apply

168 CC charging, in which a constant current is applied during the charging step and the cell voltage
169 increases over the charging duration, due to its advantage of achieving a consistent effluent salinity
170 with respect to time. To achieve a reasonable separation, the charging duration is set to 300 s, and
171 with the water recovery being fixed at 50% throughout our analysis, the discharging duration and
172 flow rate are held equivalent to that of the charging step. Additional specified parameters for the
173 MCDI modeling are provided in Table 1. Similar to Metzger et al., we consider the energy
174 consumption of MCDI both with and without energy recovery, with the dashed line representing
175 the application of energy recovery. We note that in our modeling, we rigorously calculate the
176 recoverable energy for each simulated separation, rather than use a fixed recovery ratio as assumed
177 by Metzger et al. Specifically, we calculate the recoverable energy in MCDI as the amount of
178 energy stored in the electrical double layer over the charging step minus the unavoidable resistive
179 losses during the discharging step.^{4, 20}

180 Since we maintain a constant effluent concentration of 500 ppm and a productivity of 15 L m⁻²
181 h⁻¹ across all feed salinities, a higher current density, and thus a higher average cell voltage, are
182 required as the feed salinity is increased. Consequently, \hat{E}_{fresh} increases with feed salinity, along
183 with the ultimate cell voltage (i.e. the voltage at the end of charging period). It is important to note
184 that as the cell voltage increases, so do the occurrence of Faradaic reactions (e.g. water electrolysis)
185 which cause electrode degradation and significantly detract from the current efficiency of
186 electrosorption.³⁰ Therefore, following previous theoretical and experimental studies, we constrain
187 the cell voltage to a maximum of 1.6 V, limiting the treatable feed salinities for MCDI to the lower-
188 end of the brackish water regime (<2300 ppm). Metzger et al., in contrast, seemingly do not
189 consider a maximum cell voltage, as their MCDI curve extends far past our identified practical
190 limit, into the seawater regime (up to ~40,000 ppm).

191 The MCDI curve shown in Figure 1 follows a similar trend to ED for low salinity feedwaters (i.e.,
192 <1 g L⁻¹), where the rate of growth in the specific energy consumption is large but steadies off as
193 the brackish water region is approached. This is sensible since ED and MCDI — both being
194 electro-driven technologies — incur a large potential drop from the high electrical resistance of
195 dilute solutions. Once reaching the salinity of brackish waters, the energy consumption increases
196 more linearly. We note that this linear trend is only valid for the lower end of the brackish water

197 regime we simulate, for which the effect of non-ideal co-ion leakage remains minimal. **Table 1.**
 198 Specified parameters for the RO, ED, and MCDI modeling.

Technology	Parameter	Value
RO	Feed-side mass transfer coefficient ($\text{L m}^{-2} \text{h}^{-1}$)	150
	Water permeability coefficient ($\text{L m}^{-2} \text{h}^{-1} \text{bar}^{-1}$)	3
ED	Number of cell pairs,	50
	Spacer thickness (mm)	0.3
	Membrane thickness (mm)	0.13
	Membrane charge density (mol L^{-1})	3
	Bulk diffusion coefficient of NaCl in solution ($\text{m}^2 \text{s}^{-1}$)	1.64×10^{-9}
	Effective diffusion coefficient of NaCl electromigration ($\text{m}^2 \text{s}^{-1}$)	5.15×10^{-10}
	Diffusion coefficient of NaCl in the membrane ($\text{m}^2 \text{s}^{-1}$)	1.64×10^{-10}
MCDI	Electrode macroporosity	0.43
	Electrode microporosity	0.4
	Stern layer capacitance (F mL^{-1})	120
	Specific external resistance ($\Omega \text{ cm}^2$)	30
	Specific electrode resistance ($\Omega \text{ mmol cm}^{-1}$)	0.22
	Spacer thickness (mm)	0.26
	Electrode thickness (mm)	0.29
	Membrane thickness (mm)	0.15
	Membrane charge density (mol L^{-1})	3
Bulk diffusion coefficient of NaCl in solution ($\text{m}^2 \text{s}^{-1}$)	1.64×10^{-9}	
Diffusion coefficient of NaCl in the membrane ($\text{m}^2 \text{s}^{-1}$)	1.64×10^{-10}	

199

200 The energetic performance of RO and MCDI revealed in Figure 1 is notably different than that
 201 of Metzger et al.'s Figure 6. Importantly, in Figure 1, we show that MCDI consumes more energy
 202 than RO for most of the brackish water range, being competitive only for the desalting of very
 203 dilute feeds (e.g. less than ~ 1000 ppm), for which energy consumption is very low (< 0.1 Wh/L)
 204 and thus not a primary concern. In Figure 6 of Metzger et al., however, the energy consumption of
 205 MCDI is shown to be lower than that of RO up to feed salinities above 15,000 ppm. Furthermore,

206 whereas Metzger et al. show that MCDI outperforms ED across the whole brackish water region,
207 in Figure 1 we show the opposite trend, in which the energy consumption of ED is always lower
208 than MCDI.

209 The effects of energy recovery in MCDI are also worth noting. Our results indicate that energy
210 recovery in MCDI reduces \hat{E}_{fresh} , but not significantly enough to make it more energy efficient
211 than RO or ED. Accordingly, we emphasize that the potential of energy recovery in CDI is limited,
212 as only the energy stored in the electrical double layer is theoretically recoverable, with a large
213 amount of energy irreversibly dissipating in other components of the MCDI cell (e.g. spacer
214 channel and ion-exchange membranes).^{20, 31} Though in our analysis we account for the practical
215 energy losses in both the charging and discharging steps, it is important to note that even if no
216 energy was lost in the discharging process — allowing for complete recovery of the energy in the
217 electrical double layers — the energy consumption of MCDI would remain higher than RO and
218 ED, as we have previously demonstrated.^{19, 20}

219 As highlighted by the stark difference in our Figure 1 compared to Metzger et al.'s Figure 6,
220 the authors' assessment of energy consumption is inadequate. Specifically, since the authors do
221 not hold the separation parameters and productivity consistent across all technologies, the
222 comparison of energy consumption is inherently flawed. Accordingly, the evaluation of the
223 energetic capabilities of each of the assessed technologies in the study are misleading and should
224 be reconsidered. In future technological comparisons of energy consumption, we emphasize the
225 critical need to specify the separation parameters (i.e. feed salinity, extent of salt removal, and
226 water recovery) and utilize more rigorous and mechanistic process modeling.

227

228 **Conflicts of Interest**

229 There are no conflicts to declare.

230 **Acknowledgements**

231 This work was supported by the NSF Nanosystems Engineering Research Center for
232 Nanotechnology-Enabled Water Treatment (EEC-1449500).

233 **References**

- 234 1. M. Metzger, M. M. Besli, S. Kuppan, S. Hellstrom, S. Kim, E. Sebti, C. V. Subban and J.
235 Christensen, *Energy & Environmental Science*, 2020, 13, 1544-1560.
- 236 2. S. H. Lin, *Environ Sci Technol*, 2020, 54, 76-84.
- 237 3. M. H. Sharqawy, S. M. Zubair and J. H. Lienhard, *Energy*, 2011, 36, 6617-6626.
- 238 4. L. Wang, J. Dykstra and S. Lin, *Environ Sci Technol*, 2019.
- 239 5. S. K. Patel, C. L. Ritt, A. Deshmukh, Z. X. Wang, M. H. Qin, R. Epszstein and M.
240 Elimelech, *Energy & Environmental Science*, 2020, 13, 1694-1710.
- 241 6. L. Wang, C. Violet, R. M. DuChanois and M. Elimelech, *Journal of Chemical Education*,
242 2020, DOI: 10.1021/acs.jchemed.0c01194.
- 243 7. R. Zhao, P. M. Biesheuvel and A. van der Wal, *Energy & Environmental Science*, 2012, 5,
244 9520-9527.
- 245 8. L. Wang, J. E. Dykstra and S. H. Lin, *Environ Sci Technol*, 2019, 53, 3366-3378.
- 246 9. L. Wang and S. Lin, *Water research*, 2018, 129, 394-401.
- 247 10. S. A. Hawks, A. Ramachandran, S. Porada, P. G. Campbell, M. E. Suss, P. M. Biesheuvel,
248 J. G. Santiago and M. Stadermann, *Water Research*, 2019, 152, 126-137.
- 249 11. J. J. Urban, *Joule*, 2017, 1, 665-688.
- 250 12. Y. Oren, *Desalination*, 2008, 228, 10-29.
- 251 13. M. Elimelech and W. A. Phillip, *science*, 2011, 333, 712-717.
- 252 14. R. Zhao, P. M. Biesheuvel, H. Miedema, H. Bruning and A. van der Wal, *J Phys Chem*
253 *Lett*, 2010, 1, 205-210.
- 254 15. P. M. Biesheuvel, R. Zhao, S. Porada and A. van der Wal, *Journal of Colloid and Interface*
255 *Science*, 2011, 360, 239-248.
- 256 16. P. Dlugolecki and A. van der Wal, *Environ Sci Technol*, 2013, 47, 4904-4910.
- 257 17. C. Tan, C. He, J. Fletcher and T. D. Waite, *Water Research*, 2020, 168.
- 258 18. M. E. Suss, S. Porada, X. Sun, P. M. Biesheuvel, J. Yoon and V. Presser, *Energy &*
259 *Environmental Science*, 2015, 8, 2296-2319.
- 260 19. M. Qin, A. Deshmukh, R. Epszstein, S. K. Patel, O. M. Owoseni, W. S. Walker and M.
261 Elimelech, *Desalination*, 2019, 455, 100-114.
- 262 20. S. K. Patel, M. Qin, W. S. Walker and M. Elimelech, *Environ Sci Technol*, 2020, 54, 3663-
263 3677.
- 264 21. A. Drak and M. Adato, *Desalination*, 2014, 339, 34-39.
- 265 22. T. Manth, M. Gabor and E. Oklejas, *Desalination*, 2003, 157, 9-21.
- 266 23. A. A. Sonin and R. F. Probst, *Desalination*, 1968, 5, 293-+.
- 267 24. M. Tedesco, H. V. M. Hamelers and P. M. Biesheuvel, *Journal of Membrane Science*,
268 2016, 510, 370-381.
- 269 25. M. Tedesco, H. V. M. Hamelers and P. M. Biesheuvel, *Journal of Membrane Science*,
270 2017, 531, 172-182.
- 271 26. M. Tedesco, H. V. M. Hamelers and P. M. Biesheuvel, *Journal of Membrane Science*,
272 2018, 565, 480-487.
- 273 27. W. W. Tang, P. Kovalsky, B. C. Cao, D. He and T. D. Waite, *Environ Sci Technol*, 2016,
274 50, 10570-10579.
- 275 28. P. M. Biesheuvel, Y. Q. Fu and M. Z. Bazant, *Physical Review E*, 2011, 83.
- 276 29. L. Wang and S. Lin, *Environ Sci Technol*, 2018, 52, 4051-4060.

- 277 30. C. Y. Zhang, D. He, J. X. Ma, W. W. Tang and T. D. Waite, *Water Research*, 2018, 128,
278 314-330.
279 31. L. Wang, Y. Z. Liang and L. Zhang, *Environ Sci Technol*, 2020, 54, 5874-5883.

280